Computational Mechanics (1992) 10, 397–413

Computational Mechanics

A numerical comparative study of wave propagation in inhomogeneous and random media

G. D. Manolis[1] and **A. C. Bagtzoglou**[2]

[1] Department of Civil Engineering, Aristotle University, Thessaloniki, GR 54006, Greece
[2] Center for Nuclear Waste Regulatory Analysis, Southwest Research Institute, San Antonio, Texas 78228, USA

Abstract. Continuous media through which acoustic or elastic waves propagate often exhibit inhomogeneities of various types which are difficult to describe, either due to paucity of detailed physical measurements or to the vast complexity in both space and time of these inhomogeneities. The introduction of stochasticity in the description of a continuous medium offers an attractive alternative, due to the fact that randomness is able to reproduce the wave scattering phenomena associated with a naturally occuring medium. In this work, the phenomenon of acoustic or elastic wave propagation under time harmonic conditions is used as the vehicle through which the assumption of randomness in an otherwise homogeneous medium is validated against a deterministic, inhomogeneous medium whose properties vary with depth. The range of applicability of the former model is identified through a series of parametric studies and the results are followed by a discussion on the appropriateness of the various correlation functions that can be used for representing the medium randomness. The numerical methodology employed for both deterministic and random models is a Green's function approach for waves propagating from a point source, while techniques to account for the presence of boundaries are also discussed.

1 Introduction

Wave propagation and scattering in the atmosphere, the ocean, the ground and in biological media has become very important in recent years due to widespread applications in communications, remote-sensing and detection. Natural media, however, exhibit widespread and often time-varying inhomogeneities due to the spatial dependence of their material properties. Inhomogeneity may be further accompanied by layering, anisotropy and the presence of inclusions. Furthermore, actual measurements of the particular medium properties are often obtained from small samples which are relatively homogeneous, thus masking possible abrupt changes that may occur over short distances. As a result, representing a particular medium as a homogeneous matrix over which certain properties such as density, bulk modulus, etc, exhibit a random variation is an attractive proposition requiring a rather modest effort for its description (e.g., Chernov 1962; Ishimaru 1978; Dagan 1989). It also offers a broader framework, since the restrictive assumption of homogeneity can be subsequently lifted so as to allow for material properties that are both position-dependent and random.

Problems involving a random medium are governed by stochastic differential equations. The key assumption (Barucha-Reid 1972) in the solution of such equations is the decomposition of the differential operator into a deterministic plus a random part. Then, formal inversion of the deterministic part is accomplished through the use of a Green's function and the stochastic differential equation (with its accompanying boundary conditions) can be recast as a random integral equation. A formal solution of the random integral equation can then be accomplished iteratively through use of the resolvent kernel, which in turn is defined through a Neumann series expansion. Alternatively, the dependent variable can be expanded in a general series form (Adomian 1983), and the conditions under which this expansion is equivalent to the aforementioned Neumann series or to a Born approximation are discussed in Benaroya and Rehak (1987). Finally, approximate solutions can be generated by directly applying the expectation operator to the original random integral equation and then using various closure approximations (Chernov 1962; Karal and Keller 1964; Askar and Cakmak 1988).

As far as acoustic wave propagation in a random medium is concerned, two approaches are possible, namely waves in random scatterers and waves in random continua. In the former case, the scatterer is a random distribution of many well defined particles (e.g., spheres), while in the latter case, the medium has properties which vary randomly and continuously in space (and possibly in time). Propagation of elastic and electromagnetic waves in a random, continuous medium that differs only slightly from the homogeneous case was considered by Karal and Keller (1964), using the random integral equation formulation previously alluded to. They derived an effective propagation constant which indicates that an originally coherent wave is now continuously scattered by the randomness and converted into an incoherent wave with a diminishing propagation velocity. This technique was subsequently extended to multilayered systems through the use of transfer matrices by Chu et al. (1981). Randomly layered media have also been considered in recent years by Kotulski (1990), who employed a complex transfer matrix approach in conjunction with a homogenization process to derive an equation for the effective amplitude and wavenumber of elastic waves in a stratified slab and by Kohler et al. (1991), who used asymptotic methods for stochastic differential equations to compute power spectra for receivers in a randomly layered half-space overlying a homogeneous half-space with the acoustic source placed in the latter medium. Techniques by which the probability density function, the space correlation function or other statistical measures governing wave propagation of acoustic or elastic waves in media modelled by random configurations of a large number of densely packed, identical scatteres of finite size have also been developed by, among others, Sobczyk (1976), Varadan et al. (1985), and Liu (1991).

With the exception of Pekeris (1946) solution for a point source in a layered deterministic medium with a refractive index variation proportional to the inverse of the depth, very few closed-form solutions of the inhomogeneous wave equation are available. As far as the heterogeneous Helmholtz equation governing propagation of time harmonic acoustic or horizontally polarized, elastic shear waves is concerned, we have the recent work of Li et al. (1990) who presented an exact analytic solution for a point source in a three-dimensional medium with a refractive index in the form of the square root of a simple polynomial in the depth coordinate. This work can be viewed as a generalization of earlier work of Holford (1981) for a line source extending parallel to the depth. Approximate solutions can also be generated, e.g., by decomposing the inhomogeneous medium into a stack of laterally varying layers and representing the solution within a layer as a sum of decoupled planewaves (Pai 1991). Other techniques require an a priori convenient variation of the inhomogeneity that allows for the breakdown of the solution into a general part corresponding to a differential equation with constant coefficients plus a complementary part as the sum of special mathematical functions (Shaw and Makris 1991). This latter approach is essentially a linearization procedure based on the Kirchhoff transformation that moves the nonlinearity from the governing equation to the boundary conditions (Shaw 1991). Also recently, Vrettos (1990a, 1991a) studied the eigenvalue problem and derived a Green's function for a tangential horizontal periodic line load for harmonic, horizontally polarized shear waves in a half-space with a shear modulus that exhibits an exponential, yet bounded, variation with depth. His solution for the eigenvalue problem employs the extended power series method of Frobenious, which is subsequently used to derive an integral representation for the Green's function that is solved via contour integration. This methodology was found to be applicable to the case of elastic waves in the half-plane (Vrettos 1990b) and to the axisymmetric case (i.e., the time harmonic Boussinesq solution), provided an additional step involving the Hankel transformation is taken (Vrettos 1991b).

The numerical approaches which have been used for problems involving random media are either based on boundary element-type solutions of random integral equations or on finite element-type solutions of stochastic differential operators. Both classes of numerical approaches invariably rely on a perturbation of the random medium properties. As far as boundary element solutions are concerned, we have, among others, the work of Drewniak (1985) on heat conduction problems with random heat conductivity, of Burczynski (1985) on Laplace's equation with random coefficients, of Lafe and Cheng (1987) on groundwater flow with random hydraulic conductivity and boundary conditions, and of Manolis and Shaw (1990) on acoustic wave propagation with a random wave number. In addition, there are boundary element-type applications to cases where only the excita-

tion is random, as is for instance the work of Spanos and Ghanem (1991) on continuous beams and of Luco and Wong (1986) and Pais and Kausel (1990) on rigid foundations supported on an elastic half-space.

The use of stochastic finite elements is more widespread, especially for problems in structural mechanics. Some of the basic concepts regarding discretization of the parameter space of a random field of material properties and of external loads using finite element concepts were set forth in Vanmarke et al. (1986). The basic idea behind stochastic finite elements is a Taylor series expansion of the stiffness matrix about its mean deterministic value. The major problem is of computational nature, since the computational effort increases rapidly past the second order approximation of the relevant random variables. Among the work that has been done on stochastic finite elements is that of Liu et al. (1986) on structural components, of Cruse et al. (1988) on space propulsion system components, and of Dias and Nagtegaal (1986) on fast probability integration algorithms to alleviate the high computational effort previously discussed. In general, boundary element-based stochastic analyses are more appropriate for problems involving a continuum, while their finite element counterparts are better used in problems involving structural components.

The work presented in this paper focuses on validating the assumption of randomness in describing a physical medium which exhibits a rather standard type of inhomogeneity. This is accomplished through a systematic comparison of the effects of randomness versus those of inhomogeneity on the scattering of a wave signal emanating from a point source under time harmonic conditions. For both inhomogeneous and random medium cases, a Green's function approach is employed. In the case of the random medium, a uni-variate and uni-dimensional model is used to generate realizations of its response to the wave signal, once the solution for the mean and covariance has been obtained. Also, a discussion is included on how to generalize this approach to the full spectrum of wave propagation and scattering problems. Furthermore, a systematic comparison is carried out by investigating the frequency dependence of the solutions and the relative positions of source versus receivers. Finally, various commonly used models that describe the correlation function of the wave number of the random medium are also discussed.

2 Problem statement

The governing equation for wave propagation in a three-dimensional inhomogeneous medium under time harmonic conditions is Helmholtz's equation

$$\nabla^2\varphi(\boldsymbol{x},\omega)+k^2(\boldsymbol{x})\varphi(\boldsymbol{x},\omega)=f(\boldsymbol{x},\omega) \tag{1}$$

In the above, φ is a velocity potential for acoustic waves and a displacement potential for elastic waves, f is the forcing function, $\boldsymbol{x}=(x,y,z)$ is the position vector and ω is the frequency of vibration. In addition, the wave number is $k=\omega/c$, where c is the wave propagation speed. For acoustic wave propagation, $c^2=K/\rho$ with K and ρ being the bulk modulus and the density of the medium, respectively. For elastic wave propagation, $c^2=(\lambda+2\mu)/\rho$ for the case of longitudinal (pressure) waves and $c^2=\mu/\rho$ for the case of transverse (shear) waves, with λ and μ being the Lamé constants (Manolis and Beskos 1988). Actually, a change of variables involving scaling of the potential φ has already taken place in conjunction with Eq. (1) (Shaw and Makris 1991) so as to deal with the combined effect of inhomogeneity which, from a physical point of view, occurs in both the modulus and the density of the medium.

The usual homogeneous type of boundary conditions associated with Eq. (1) are

$$\varphi=0 \text{ on } S_1 \quad \text{and} \quad \partial\varphi/\partial n=0 \text{ on } S_2 \tag{2a, b}$$

where $S=S_1+S_2$ is the total surface and n is the outward pointing, unit normal on S. For acoustic waves, Eqs. (2a) and (2b) respectively denote a free boundary and a rigid boundary. For elastic waves, the aforementioned equations respectively denote a rigid surface and a traction-free surface. Furthermore, in the presence of unbounded media the scattered waves must obey the radiation condition, i.e.,

$$\varphi=0 \quad \text{for} \quad \boldsymbol{x}\to\infty \tag{2c}$$

3 Inhomogeneous medium

Solutions to Eq. (1) are known only for specific forms of $k(x)$ (Li et al. 1990). We will consider here the case

$$k(z) = k_0(1 + Az)^{1/2}, \tag{3}$$

where k_0 is the reference homogeneous medium's wave number. The above expression corresponds to a wave number whose square increases linearly with depth when parameter A is negative, as shown in Fig. 1. The rate of increase depends on the particular value of A, and for $A = 0$ the homogeneous case is recovered. This type of inhomogeneity physically corresponds to the case where either the medium's density or its elastic constant (or possibly both) vary in such a way so that their combined effect can be represented by Eq. (3). Thus, there exists a physical reason for generating a random, spatially correlated representation for the wave number in the next section.

The displacement at receiver $\boldsymbol{r}$ in the inhomogeneous medium described by Eq. (3) resulting from a point source of unit strength at location $\boldsymbol{r}_s$ is labeled as the Green's function $G(\boldsymbol{r}, \boldsymbol{r}_s)$ and is the solution of Eq. (1) for $f = -\delta(\boldsymbol{r}, \boldsymbol{r}_s)$, where δ is the Dirac delta function. A closed-form solution for G for the case of three-dimensional acoustic wave propagation and obeying the radiation condition given by Eq. (2c) was recently obtained by Li et al. (1990) working in spherical coordinates as

$$G(\boldsymbol{r}, \boldsymbol{r}_s) = \frac{-\exp(\mathrm{i}\pi/6)}{2R}\{Ai'(a)Ai(b) - \exp(\mathrm{i}2\pi/3)Ai(a)Ai'(b)\}. \tag{4}$$

In the above, $R = |\boldsymbol{r} - \boldsymbol{r}_s|$ is the distance between receiver and source points and Ai is Airy's function with the prime denoting derivative with respect to the argument.

The two arguments appearing above are

$$a = -\left(\frac{k_0}{A}\right)^{2/3}\left(1 + \frac{A}{2}(z + z_s) - \frac{|A|R}{2}\right) \quad \text{and} \quad b = -\exp(\mathrm{i}2\pi/3)\left(\frac{k_0}{A}\right)^{2/3}\left(1 + \frac{A}{2}(z + z_s) + \frac{|A|R}{2}\right), \tag{5}$$

where k_0 is the homogeneous wave number and z and z_s are the depth of the receiver and source, respectively.

As noted before, parameter A controls the degree of inhomogeneity and that for $A = 0$, Eq. (4) reduces to the homogeneous Green's function

$$G_h(\boldsymbol{r}, \boldsymbol{r}_s) = \frac{\exp(\mathrm{i}k_0 R)}{4\pi R}. \tag{6}$$

It should be noted that the Airy functions remain bounded as their argument goes to zero (McLachlan 1954). As a result, the inhomogeneous Green's function exhibits the well known $1/R$

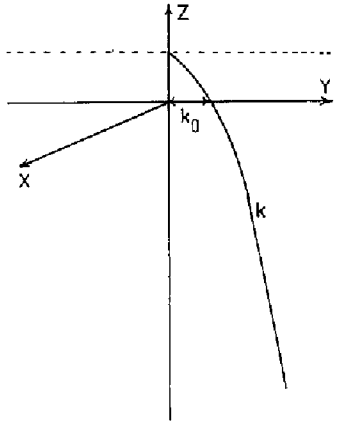

Fig. 1. Inhomogeneous medium with wave number $k = k_0\sqrt{1 + Az}$

singularity, which is typical of fundamental solutions corresponding to elliptic and hyperbolic differential operators for three-dimensional problems. Finally, in order to recover Green's functions which are able to reproduce the boundary conditions of either a free or a rigid horizontal surface (see Eqs. 2), the general method of images may be used as discussed in Appendix A.

4 Stochastic medium

In the case of a stochastic medium, the wave number becomes a random variable given by

$$k(\gamma) = k_0 + \varepsilon k_1(\gamma) + \varepsilon^2 k_2(\gamma) + \cdots, \tag{7}$$

where k_0 is the mean wave number for the homogeneous case and $k_1, k_2, \ldots$ are random fluctuations about the mean. Also, γ is a random parameter and ε is the perturbation parameter which is assumed to be small compared to unity. The randomness in the wave number can be thought of as a manifestation of randomness in the density and/or the elastic modulus, and is depicted in Fig. 2.

A consequence of medium randomness is that the response is also random and can be expanded using perturbation about the mean value φ_0 as

$$\varphi(\boldsymbol{x}, \omega, \gamma) = \varphi_0(\boldsymbol{x}, \omega) + \varepsilon\varphi_1(\boldsymbol{x}, \omega, \gamma) + \varepsilon^2\varphi_2(\boldsymbol{x}, \omega, \gamma) + \cdots. \tag{8}$$

It is noted that the mean response is deterministic and corresponds to the homogeneous medium case.

For a point source placed at $\boldsymbol{r}_s$, the response $\varphi(\boldsymbol{x}, \gamma)$ can be identified with the random Green's function $G_r(\boldsymbol{r}, \boldsymbol{r}_s, \gamma)$, which is the solution of Eq. (1) with $k(z)$ replaced by $k(\gamma)$ and with $f(\boldsymbol{x}, \omega)$ being the usual unit point source. Since $k(\gamma)$ corresponds to a homogeneous, yet random, medium G_r has the same form as G_h given by Eq. (6) with k_0 replaced by $k(\gamma)$. A perturbation expansion can now be written for G_r (Manolis and Shaw 1990, 1992) as follows

$$G_r(R, \gamma) = \frac{\exp(\mathrm{i}k(\gamma)R)}{4\pi R} = G_0(R) + \varepsilon G_1(R, \gamma) + \varepsilon^2 G_2(R, \gamma) + \cdots$$

$$= \frac{1}{4\pi R}\exp(\mathrm{i}k_0 R)\{1 + \mathrm{i}\varepsilon k_1 R + (\mathrm{i}\varepsilon k_1 R)^2/2\} + \cdots, \tag{9}$$

where $R = |\boldsymbol{r} - \boldsymbol{r}_s|$ as before. The zeroth and first order terms of the above expression are

$$G_0(R) = G_h(R) \quad \text{and} \quad G_1(R, \gamma) = \mathrm{i}k_1(\gamma)\exp(\mathrm{i}k_0 R)/4\pi \tag{10a, b}$$

respectively.

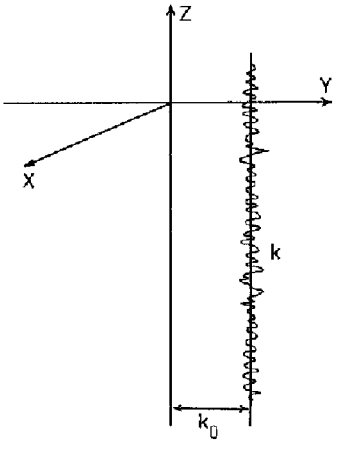

Figs. 2. Medium exhibiting a random variation of the wave number k

At this stage, it is necessary to introduce the expectation operator E, which denotes statistical averaging. By applying the expectation to Eq. (9), we have that

$$E\{G_r(R,\gamma)\} = \langle G_0(R)\rangle = m_G = G_0(R) \tag{11}$$

indicating that the mean solution corresponds to the deterministic, homogeneous medium case. This result is a consequence of the assumption that the higher order terms in Eq. (9) are zero-mean random process. Next, the covariance of the response is obtained as

$$E\{G_r(R_i,\gamma)G_r(R_j,\gamma)\} = K_G = G_0(R_i)G_0(R_j) + \varepsilon^2\langle G_1(R_i)G_1(R_j)\rangle \tag{12}$$

where R_i and R_j indicate two different radial distance values. By substituting in the above the expressions for G_0 and G_1 given by Eqs. (10), the following closed-form expression is obtained for the covariance of the response

$$K_G = \frac{\exp(ik_0(R_i+R_j))}{(4\pi)^2}\left\{\frac{1}{R_iR_j} - \varepsilon^2\langle k_1^2(\gamma)\rangle\right\}. \tag{13}$$

The particular form of K_G now depends on the correlation function of $k_1^2(\gamma)$. The following models are commonly used in the literature (e.g., Dagan 1989)

1) Exponential function, where

$$\langle k_1^2(\gamma)\rangle = \sigma_k^2\exp(-|\xi|/\lambda_k) \tag{14}$$

with σ_k^2 the variance of k_1, λ_K the correlation length and $\xi = R_j - R_i$

2) Delta function, where

$$\langle k_1^2(\gamma)\rangle = \sigma_k^2\delta(\xi) \tag{15}$$

and

3) Piecewise linear function, where

$$\langle k_1^2(\gamma)\rangle = \sigma_k^2(1-|\xi|/\lambda_k) \quad \text{if} \quad |\xi| < \lambda_k \tag{16}$$

and zero otherwise. It should be noted that the present stochastic model, whereby randomness is superimposed on an otherwise homogeneous medium, is somewhat simple. As such, this model should be viewed as a "first-order" model that serves as a stepping stone towards a more refined model with randomness superimposed on position-dependent properties (e.g., Hryniewicz 1991).

5 Stochastic field simulations

Once the mean m_G and the covariance K_G of the response have been determined, it is possible to obtain a realization of the random field $\varphi(x,\omega,\gamma)$ (here represented by the Green's function $G_r(R,\gamma)$) by assuming that it is a uni-dimensional, uni-variate stochastic process. Such a procedure (Shinozuka 1972; Vanmarke et al. 1986) requires use of the Fourier transform. We begin by defining a zero-mean random field

$$G_r'(R,\gamma) = G_r(R,\gamma) - G_0(R,\gamma) \tag{17}$$

so that $m_{G'} = 0$ and the covariance is, for an exponential correlation function,

$$K_{G'}(\xi) = -\varepsilon^2\sigma_k^2\exp(ik_0(2R+\xi))\exp(-|\xi|/\lambda_K)/(4\pi)^2. \tag{18}$$

The above expression is a function of the relative distance ξ between two receivers and, as such, is the autocovariance of $G_r'(R,\gamma)$.

It is well known that the autocovariance function $K_{G'}(\xi)$ and the power spectral density function (PSDF) $S_{G'}(s)$ from a Fourier transform pair, i.e.,

$$S_{G'}(s) = \frac{1}{2\pi}\int_{-\infty}^{\infty} K_{G'}(\xi)\exp(-is\xi)d\xi \quad \text{and} \quad K_{G'}(\xi) = \int_{-\infty}^{\infty} S_{G'}(s)\exp(+is\xi)ds, \tag{19a, b}$$

where s is the Fourier transform parameter corresponding to ξ. Once the direct transform of Eq. (19a) has been performed, usually numerically, then the realization of the random motion $G'(R,\gamma)$ is given (Shinozuka 1972) as follows

$$\tilde{G}'_c(R) = \sqrt{2} \sum_{j=i}^{N} c_j \cos(s_j R + \phi_j), \tag{20}$$

where

$$c_j = \sqrt{2S_{G'}(s_j)\Delta s} \quad \text{and} \quad s_j = j\Delta s. \tag{21a, b}$$

In the above, Δs is the increment in s and ϕ_j is a random phase angle which is uniformly distributed in the interval $(0,2\pi)$. As the number of samples N increases, the realization $\tilde{G}'_c$ becomes a more realistic representation of the original random variable G'. Furthermore, the envelope $\tilde{G}'_e$ of the random vibration can be found as

$$\tilde{G}'_e(R) = ((\tilde{G}'_c(R))^2 + (\tilde{G}'_s(R))^2)^{1/2}, \tag{22}$$

where realization $\tilde{G}'_s$ is given by Eqs. (20) and (21) with the cosine replaced by a sine. Finally, all that remains to be done is to add the mean m_G to the above realizations.

The PSDF can be found in closed form for the case of an exponential correlation for $k_1(\gamma)$ (see Eq. 18) as

$$S_{G'}(s) = \frac{Z}{\pi} \frac{1/\lambda_k}{(1/\lambda_k^2 + (k_0 - s)^2)}, \tag{23}$$

where

$$Z = -\varepsilon^2 \sigma_K^2 \exp(\mathrm{i}2k_0 R)/(4\pi)^2. \tag{24}$$

For the case of a delta correlation (see Eq. 15), we have a constant PSDF in s, i.e.,

$$S_{G'}(s) = Z/(2\pi) \tag{25}$$

and for other types of correlation functions, such as the piecewise linear function of Eq. (16), standard discrete fast Fourier transform (FFT) algorithms can be used. Care must be excercised, however, because most discrete FFT algorithms consider only the positive range 0 to $N\Delta s$, where $\Delta s = 2\pi/(N\Delta\xi)$, with N the total number of samples. This poses a problem because for a complex-valued function such as $K_{G'}(\xi)$, different expressions are obtained by integrating from 0 to $+\infty$ and doubling the result as compared to integrating from $-\infty$ to $+\infty$. Furthermore, $S_{G'}(s)$ is not always an even function of s as is usually pre-supposed by the realization process of Eqs. (19)–(22). As a result, it is necessary to sample $S_{G'}(s)$ along both negative and positive values of s_j and omit the factor of two in Eq. 21(a).

6 Numerical simulations

In this section, we will first examine the propagation patterns of a shear wave in the inhomogeneous three-dimensional continuum of Fig. 1 and subsequently in the random homogeneous three-dimensional continuum of Fig. 2. Finally, a comparison between these two models will be made so as to ascertain the range, in terms of distance, orientation and frequency, over which the stochastic model can reproduce wave propagation phenomena associated with medium inhomogeneity.

6.1 Inhomogeneous medium

Consider the inhomogeneous medium of Fig. 1, where the wave number is a function of depth as given by Eq. (3). We will consider an average shear wave velocity $c = 4.62$ km/sec, which is typical of firm ground (Chu et al. 1981). Three forcing frequencies are studied, namely $\omega = 4.62\, r/s$ (0.74 Hz),

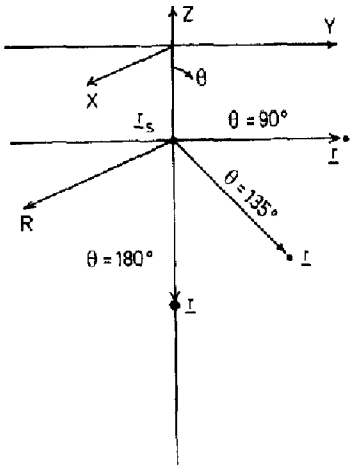

Fig. 3. Source at r_s and receiver r along lines forming an angle θ with respect to the vertical

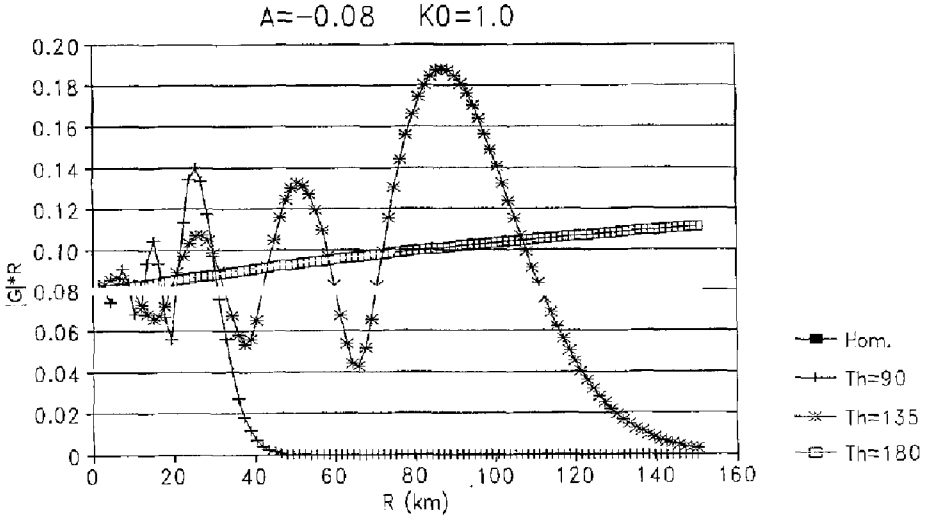

Fig. 4. Dimensionless wave amplitude versus radial distance in an inhomogeneous medium for $k_0 = 1.0\,\mathrm{km}^{-1}$ and source depth of 15 km

18.48 r/s (2.94 Hz) and 73.92 r/s (11.76 Hz). In view of the fact that the instruments for recording seismic motions operate in the band 0.5 to 25.0 Hz, the above values respectively represent wave propagation in the low, intermediate and high frequency ranges and result in reference wave number k_0 values of 1.0, 4.0 and 16.0 km^{-1}. The constant A in Eq. (3) is taken as equal to -0.08, which means that the turning point above which k is negative is 12.5 km along the z-axis. If this point is taken as the location of the horizontal free surface, then a point source at $z = -2.5$ km is actually buried 15 km below the surface. We will thus ignore the effects of the free surface, although these can be accounted for as discussed in Appendix A. As shown in Fig. 3, receivers are placed along lines forming an angle $\theta = 90°$, 135° and 180° with respect to the vertical axis. These receivers are equally spaced every 1.5 km and span a distance of 150 km, i.e., ten times the source depth. It is noted in passing that the minimum time required for the transient shear wave signal to be reflected from the free surface and reach the receiver line is 6.4 seconds.

Figures 4 through 6 plot the normalized wave amplitude versus radial distance R from the source for reference wave number k_0 values of 1.0, 4.0 and 16.0 km^{-1}, respectively. It is noted that the shear wave displacement potential φ is identified with the Green's function G of Eq. (4), which

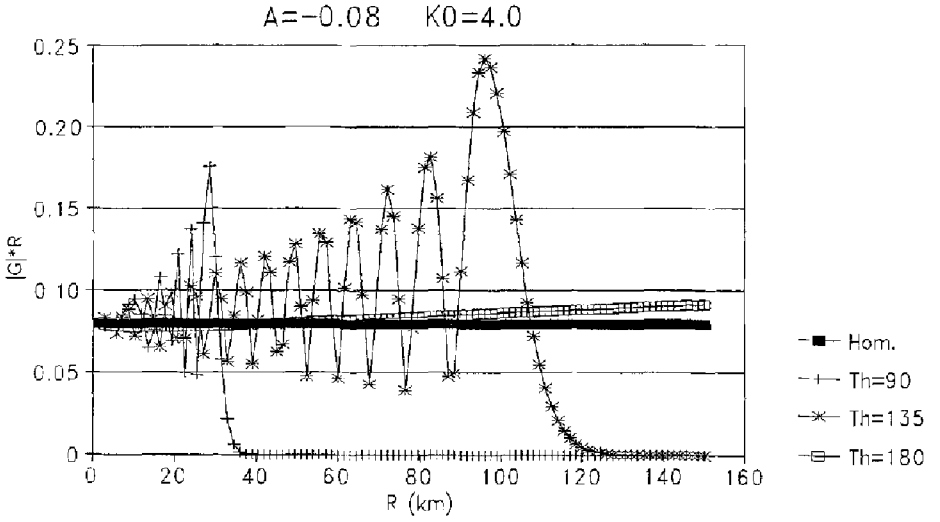

Fig. 5. Dimensionless wave amplitude versus radial distance in an inhomogeneous medium for $k_0 = 4.0\,\mathrm{km}^{-1}$ and source depth of 15 km

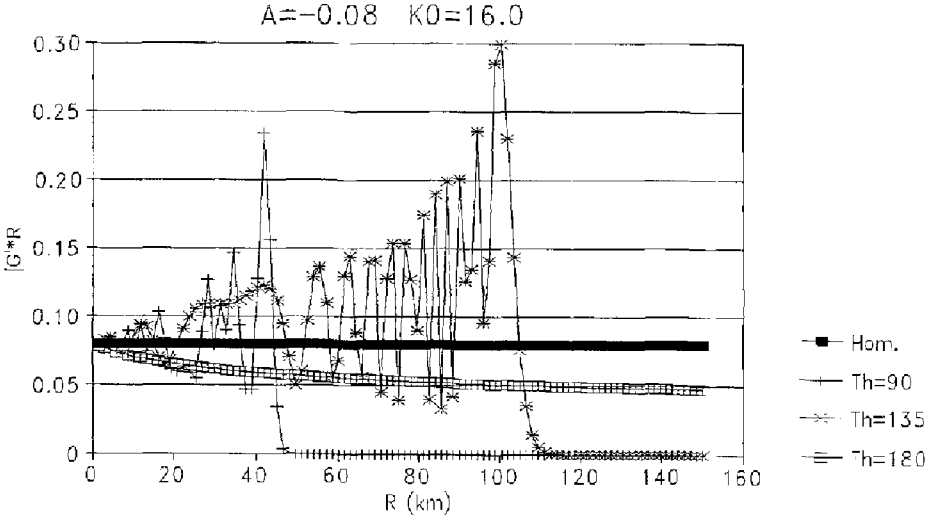

Fig. 6. Dimensionless wave amplitude versus radial distance in an inhomogeneous medium for $k_0 = 16.0\,\mathrm{km}^{-1}$ and source depth of 15 km

is a complex variable. In all cases, the solution for the homogeneous case $A = 0$, i.e. Eq. (6), is plotted as the reference curve. The accuracy of the numerical implementation of Eq. (4) has been verified through comparisons with the results available in Li et al. (1990).

With reference to Figs. 4–6, we first note that very close to the source, the normalized amplitude $|G|R$ is constant, indicating that the wave amplitude decreases proportionally to $1/R$, as is the case for the homogeneous medium. For R in the neighborhood of a few km from the source, the amplitude decreases much more rapidly than $1/R$, and the rate of decrease depends on the angle θ. The location of the rapid drop is around $R = 40\,\mathrm{km}$ and 110 km for $\theta = 90°$ and $\theta = 135°$, respectively, which marks the transition zone (caustic boundary) between illuminated and shadow zones. Note that the location of these turning points remains unchanged as the forcing frequency ω increases. Classic ray theory (e.g., Pekeris 1946) predicts the existence of a shadow zone of zero strength in an unbounded inhomogeneous medium, since rays are confined to the illuminated side

of the caustic boundary. The line $\theta = 180°$ never crosses a caustic boundary and, as a result, relatively small differences with respect to the solution for the homogeneous medium are noticed, which become progressively smaller at higher wave numbers (or higher forcing frequencies). Furthermore, the wave amplitude oscillations observed at $\theta = 90°$ and 135° become very pronounced as the wave number k_0 (or ω) increases. These oscillations are formed because of interference between the original incident wave and the wave reflected from the turning point (Li et al. 1990).

6.2 *Stochastic medium*

The stochastic medium of Fig. 2 has the same mean shear wave velocity, source-receiver topology and is under the same forcing frequencies ω as the inhomogeneous medium of the previous section. The orientation of the line along which the receivers are placed, however, is irrelevant since the stochastic medium is modelled as a small perturbation against a homogeneous background and since the presence of a free surface is ignored. The stochasticity in the wave number $k(\gamma)$ is modelled via the correlation functions of Eqs. (14)–(16). The variance σ_k^2, which is the value of the correlation function at distance $\xi = 0$ from a given receiver, is taken as equal to $0.25\,\text{km}^{-2}$. This number is within the low range of values considered acceptable for typical applications (Chu et al. 1981). Reasonable values for the correlation length λ_k are in the order of a few hundred meters (Chu et al. 1981). We note that for an exponential correlation function, the resulting PSDF of the autocovariance function $K_{G'}(\xi)$ is not an even function of the transform parameter s. This can be ascertained by inspection of Eq. (23) and is due to the fact that $K_{G'}(\xi)$ is a complex function. The implication of this is that sampling of the one-sided PSDF along positive values of s, as required by Eqs. (20) and (21), is only acceptable at very low values of k_0 (or ω), since the PSDF is even about k_0. For higher values of k_0, it is necessary to sample the two-sided PSDF along both negative and positive values of s.

Figures 7 through 9 present parametric studies that investigate the effect of λ_k and σ_k^2 on the stochastic realization of the wave displacement amplitude $|G|$ for the case of an exponential correlation function for $k_1(\gamma)$. The stochastic realization is in the form of an unscaled ($\varepsilon = 1.0$) envelope (see Eq. 22) and is for the low wave number value of 1.0. Higher values of k_0 do not so much affect the magnitude of the envelope as they do its "frequency" s content, as can be seen by recourse to the form of $K_G(\xi)$ in Eq. (23). The sampling interval $\Delta\xi$ of ξ does not enter the generation of the envelope since the PSDF is obtained in closed form. Only if the PSDF must be obtained numerically via the FFT (see Eq. 19) is $\Delta\xi$ needed, and then its magnitude should be comparable to that used

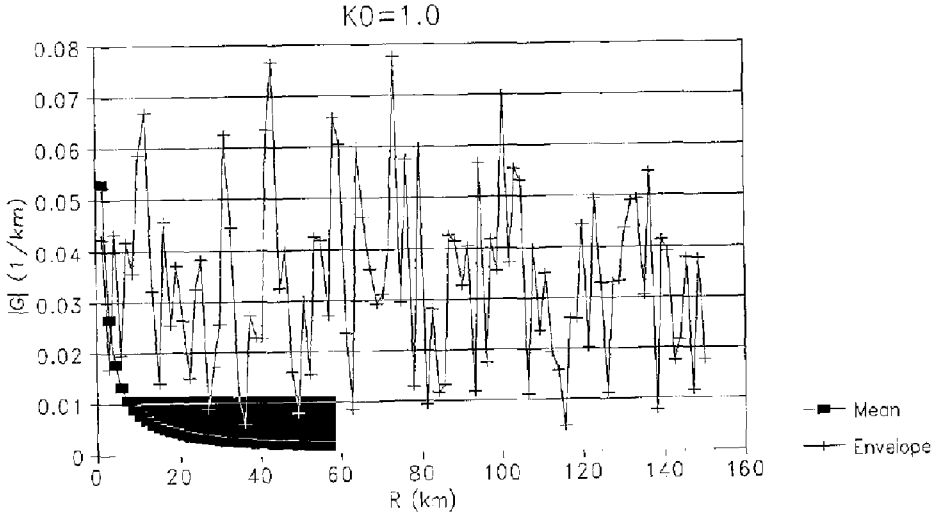

Fig. 7. Mean and envelope of wave motion at $k_0 = 1.0\,\text{km}^{-1}$ for exponential correlation with $\sigma_k^2 = 0.25\,\text{km}^{-2}$ and $\lambda_k = 0.10\,\text{km}$

for λ_k. In all cases, the amplitude of the mean (average solution) is included as the reference solution, and the receivers range from 0 to 150 km in equal increments of 1.5 km. The mean solution, as expected, decreases exponentially rather rapidly with distance from the source and is imperceptible past a distance of 40 km.

It is first observed in Figs. 7 and 8 that the unscaled envelope is essentially bounded in the interval 0.02 to 0.08 km^{-1} and exhibits a few peaks below and above those bounds. As λ_k increases, the aforementioned peaks increase in magnitude and the envelope becomes less "noisy", a fact consistent with previous observations (Bagtzoglou 1990). Finally, by comparing Figs. 7 and 8 with Fig. 9, we see that the standard deviation σ_k^2 simply acts as a scaling factor for the envelope. This is a consequence of the simplicity of the model, i.e., a perturbation of the wave number seen against a homogeneous medium background. It should be added that the number of samples N in Eq. (20) is kept at 256, which is considered adequate in view of the fact that any further increase of N at fixed R and ϕ_j does not appreciably change the results.

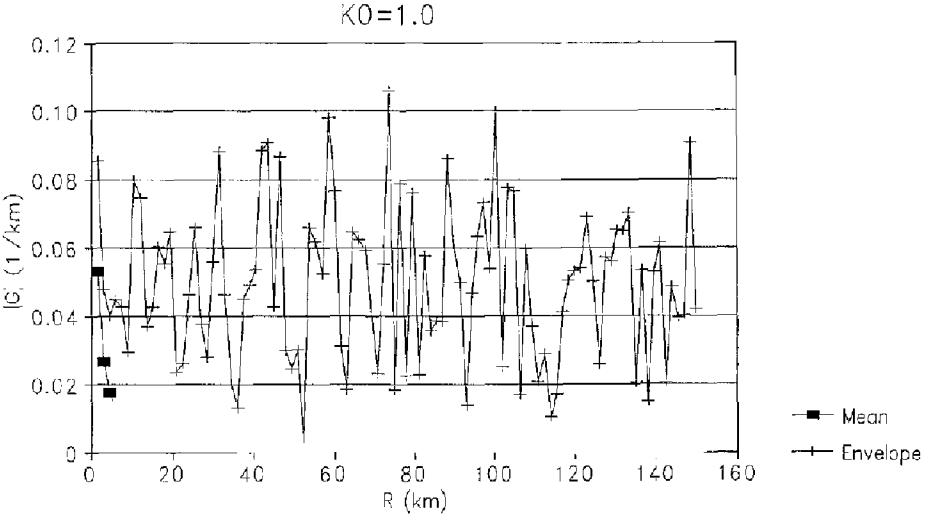

Fig. 8. Mean and envelope of wave motion at $k_0 = 1.0\,km^{-1}$ for exponential correlation with $\sigma_k^2 = 0.25\,km^{-2}$ and $\lambda_k = 0.80\,km$

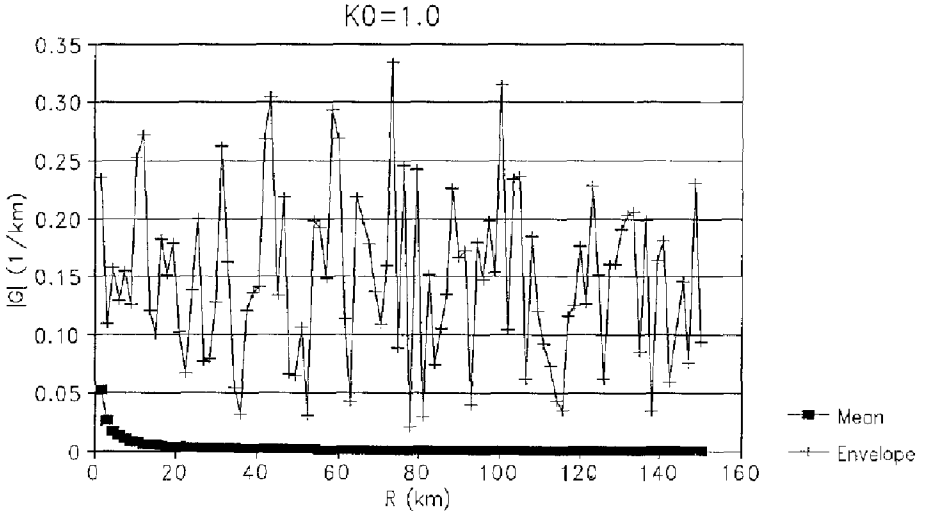

Fig. 9. Mean and envelope of wave motion at $k_0 = 1.0\,km^{-1}$ for exponential correlation with $\sigma_k^2 = 0.25\,km^{-2}$ and $\lambda_k = 0.40\,km$

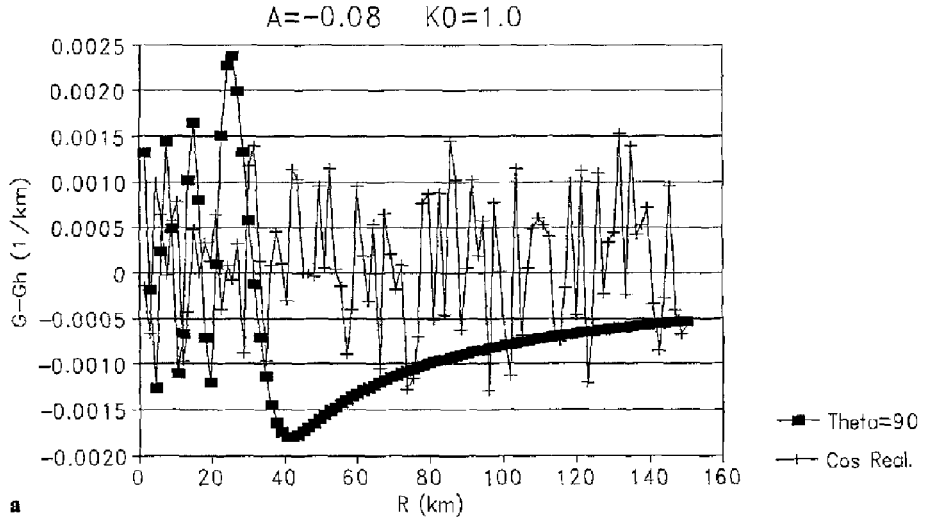

a

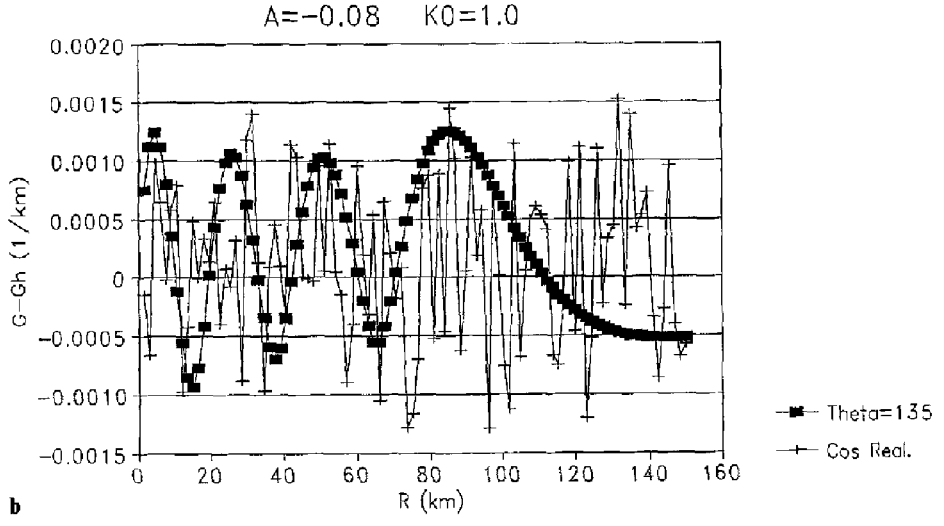

b

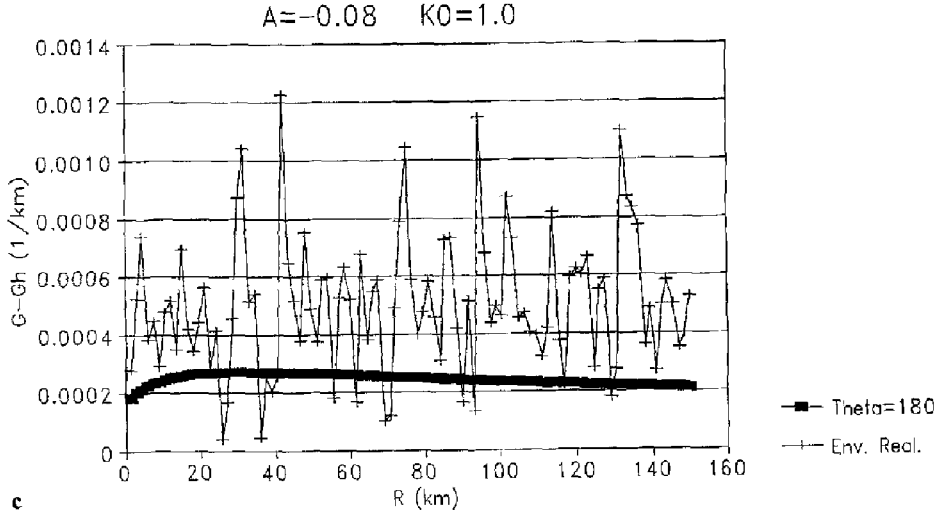

c

Fig. 10. Comparison between inhomogeneity and randomness with respect to the wave motion amplitude at $k_0 = 1.0\,\mathrm{km}^{-1}$ along the lines **a** $\theta = 90°$, **b** $\theta = 135°$ and **c** $\theta = 180°$

The piecewise linear correlation function of Eq. (16) for $\Delta\xi \cong \lambda_k$ gives similar results to the exponential correlation function discussed above and will not be pursued further. The delta correlation function of Eq. (15) results in a constant PSDF. As such, this model is very susceptible to the sampling rate s_j and results in envelope functions that are unacceptably large compared to the ones obtained from the exponential correlation. Therefore, only the exponential correlation model will be subsequently retained with $\sigma_k^2 = 0.25\,\mathrm{km}^{-2}$ and $\lambda_k = 0.40\,\mathrm{km}$.

6.3 Comparison study

In this section, the results of the stochastic realization process previously described will be used, after appropriate scaling, to simulate the effect that wave number inhomogeneity has on propagating shear waves. To that effect, Figs. 10–12 plot the difference in the wave amplitude between the inhomogeneous (G) and homogeneous (G_h) cases versus radial distance R from the source at k_0 values of 1.0, 4.0 and 16.0 km^{-1}, respectively. Concurrently plotted are the results of the stochastic realization process in the form of a cosine realization (Eq. 20) for lines $\theta = 90°$ and 135° and in the

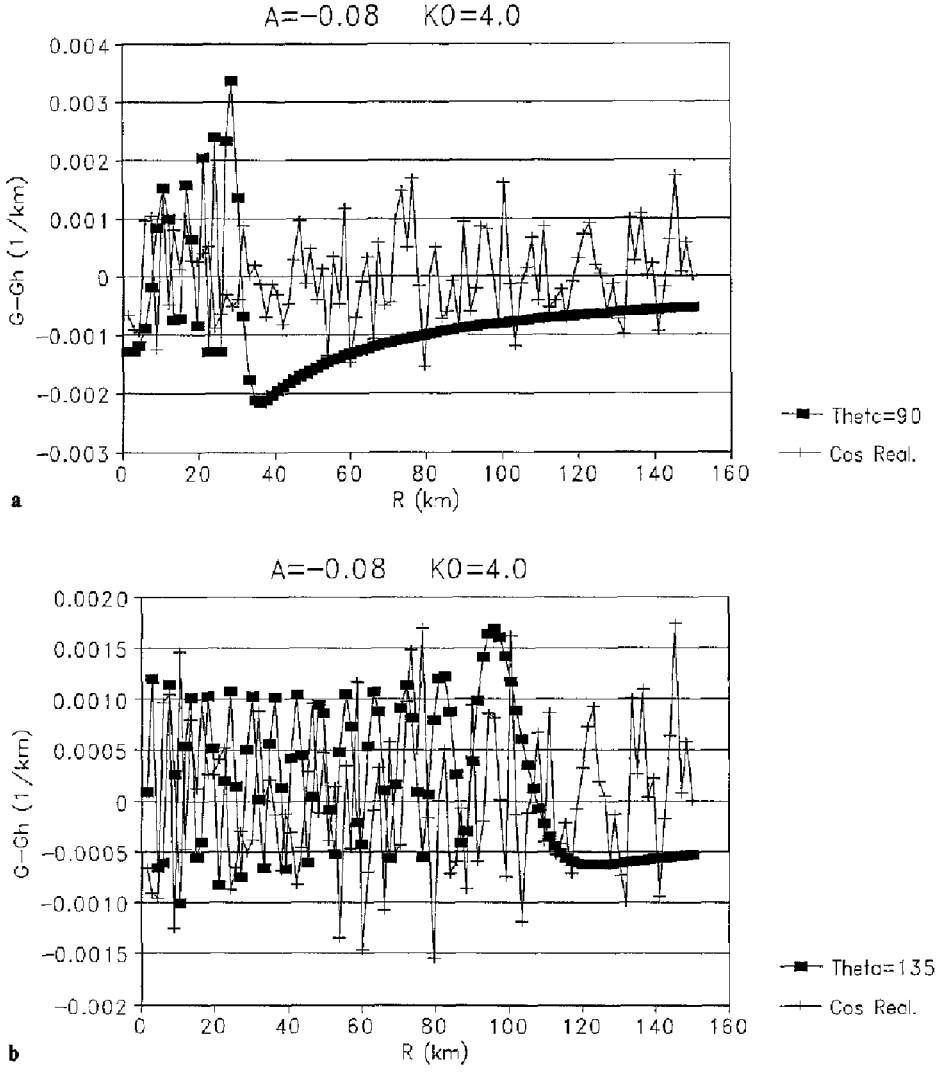

Fig. 11. Comparison between inhomogeneity and randomness with respect to the wave motion amplitude at $k_0 = 4.0\,\mathrm{km}^{-1}$ along the lines **a** $\theta = 90°$ and **b** $\theta = 135°$

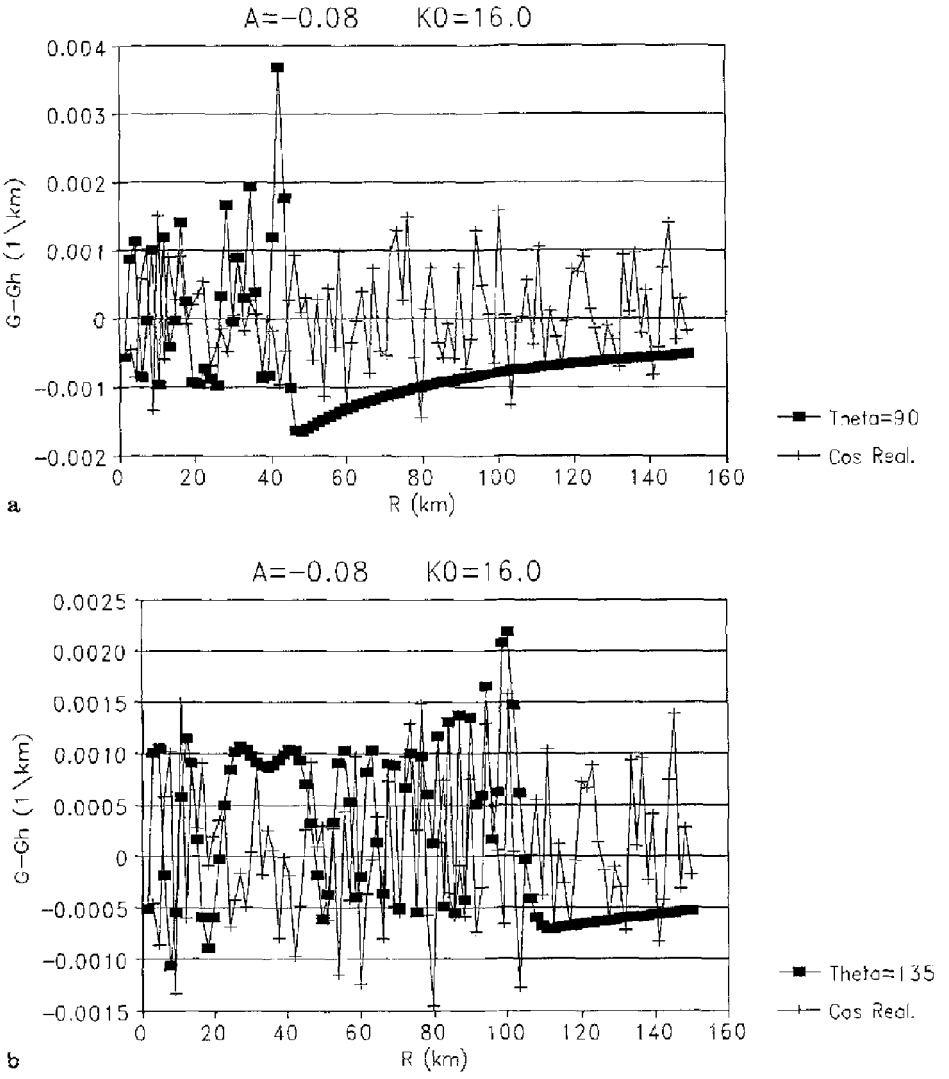

Fig. 12. Comparison between inhomogeneity and randomness with respect to the wave motion amplitude at $k_0 = 16.0\,\mathrm{km}^{-1}$ along the lines **a** $\theta = 90°$ and **b** $\theta = 135°$

form of an envelope (Eq. 22) for the line $\theta = 180°$ in Fig. 10c. The choice of an envelope, which is always positive, is dictated by the fact that the difference $G - G_h$ along $\theta = 180°$ does not oscillated about zero since that line never crosses a caustic boundary. The results of the stochastic realization process have been divide by 50, which corresponds to a scaling $\varepsilon = \sqrt{50} = 7.1$, for the low and intermediate wave numbers. For the high wave number, the scaling factor is $\varepsilon = \sqrt{20} = 4.5$.

With the exception of the line $\theta = 180°$, the stochastic model is able to capture rather well the effect of inhomogeneity along the lines $\theta = 90°$ and $\theta = 135°$ and for all k_0. The stochastic simulation is always better up to a distance which coincides with the location of the caustic boundary, i.e., R around 40 km for the line $\theta = 90°$ and R around 110 km for the line $\theta = 135°$. The reason is, of course, that the wave amplitude oscillates prior to approaching a caustic boundary and then drops to very low values, as was discussed in Sect. 6.1. Furthermore, the stochastic simulation is better at $k_0 = 16.0$ compared to $k_0 = 1.0$, which implies that the realization process becomes better as the forcing frequency increases. Finally, the line $\theta = 80°$ can only be qualitatively modelled by the stochastic envelope, because of the fact that the inhomogeneous medium solution differs little from the corresponding homogeneous one.

7 Conclusions

This work investigated the validity of a homogeneous, stochastic medium model as a way of representing wave propagation patterns associated with an inhomogeneous medium exhibiting a depth-dependent wave number. The focus was on shear wave propagation under time harmonic conditions. For a typical point source-receiver configuration and for parameter values considered representative to this problem, the numerical stochastic realizations were able to reproduce the correct wave patterns for (a) wave number values of 1.0 to 16.0 km^{-1}, which indicates that the entire frequency range of interest of 0.5 to 25.0 Hz can be captured and (b) radial distances within the "illuminated" zone for a particular line of receivers. For receivers in the shadow zone, stochastic realizations give only a rough qualitative picture of the wave patterns occuring there.

Acknowledgements

The first author would like to acknowledge the NATO International Scientific Exchange Program for Collaborative Research Grant No. CRG 91-4033, which has made possible a very fruitful exchange of ideas with Prof. R. P. Shaw of the State University of New York at Buffalo. Mrs. V. Baxevani is also acknowledged for typing the manuscript.

Appendix A—Method of Images

It is well known (e.g., Mindlin (1936) in elastostatics) that in order to recover a Green's function G_h^* that can reproduce the boundary conditions for either a free or a rigid horizontal surface, the method of images which requires placing a unit point source at image point r_s^i as shown in Fig. 13, may be used. In particular, the two sources (original and image) are subtracted as

$$G_h^*(r, r_s, r_s^i) = G_h(r, r_s) - G_h(r, r_s^i) \tag{A1}$$

for the case of an acoustically free horizontal boundary and are added as

$$G_h^*(r, r_s, r_s^i) = G_h(r, r_s) + G_h(r, r_s^i) \tag{A2}$$

for the case of an acoustically rigid horizontal boundary, where G_h is the Green's function of Eq. (6) for the homogeneous fullspace. It is easy to see that the boundary condition for the free surface in Eq. (2a) is correctly reproduced by Eq. (A1) since along the horizontal surface the following conditions hold

$$r = (x, y, 0), \quad r_s = (x_s, y_s, -z_s), \quad r_s^i = (x_s, y_s, z_s),$$
$$R = |r - r_s| = R^i = |r_s - r_s^i| = [(x - x_s)^2 + (y - y_s)^2 + z_s^2]^{1/2}. \tag{A3}$$

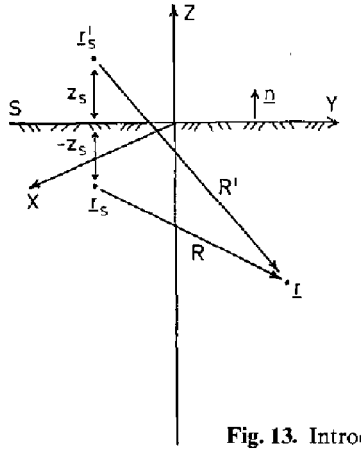

Fig. 13. Introduction of image source r_s^i to compensate for the presence of the free surface along $z = 0$

Furthermore, the normal derivative of G_h is given by the chain rule as

$$\frac{\partial G_h}{\partial n} = \frac{\partial G_h}{\partial R}\frac{\partial R}{\partial n} = \frac{\exp(ik_0 R)}{4\pi R}(ik_0 - 1/R)\frac{\partial R}{\partial n}. \tag{A4}$$

When expressions such as the above are taken into account in Eq. (A2), along with the condition that across the horizontal surface

$$\frac{\partial R}{\partial n} = -\frac{\partial R^i}{\partial n} = \frac{z_s}{R}, \tag{A5}$$

then the condition for the rigid surface given by Eq. (2b) is correctly reproduced.

With regards to the inhomogeneous case, superposition of the original and image sources is not sufficient for reproducing either a free or a rigid horizontal boundary, due to the explicit presence of the z_s coordinate of the source in the arguments of the Airy functions (see Eqs. 4 and 5). However, superposition of the original unit point source for a given value of A at $\boldsymbol{r}_s$ with a unit point source for $-A$ at $\boldsymbol{r}_s^i$ works. Consider first the acoustically free horizontal surface, where

$$G^*(R, R^i, a, a^i, b, b^i) = G(R, a(A), b(A)) - G(R^i, a^i(-A), b^i(-A)) \tag{A6}$$

with G given by Eq. (4). Along the horizontal surface, Eqs. (A3) hold and, as a result,

$$a = -\left(\frac{k_0}{A}\right)^{2/3}\left(1 + \frac{A}{2}(-z_s) - \frac{|A|R}{2}\right) = a^i = -\left(\frac{k_0}{-A}\right)^{2/3}\left(1 + \frac{(-A)}{2}(z_s) - \frac{|-A|R}{2}\right). \tag{A7}$$

Similarly, $b = b^i$ when $z = 0$. Consequently, Eq. (A6) goes to zero and thus the boundary condition of Eq. (2a) is reproduced.

As far as the acoustically rigid horizontal surface is concerned, the appropriate Green's function is Eq. (A6) with a positive sign. To assure satisfaction of Eq. (2b), consider the normal derivative of $G(R, a, b)$

$$\frac{\partial G}{\partial n} = \frac{\partial G}{\partial R}\frac{\partial R}{\partial n} = \frac{\exp(i\pi/6)}{2}\frac{\partial R}{\partial n}\left\{\frac{1}{R^2}g(a(A), b(A)) - \frac{1}{R}\frac{\partial g(a(A), b(A))}{\partial R}\right\}, \tag{A8}$$

where g represents the terms in the curly bracketts in Eq. (4) involving the Airy functions Ai and Ai'. Since there exists a recursive formula for evaluating the derivatives of the Airy functions (Mc Lachlan 1954), the expression $\partial g/\partial R$ inside the curly bracketts in the above equation can be evaluated in closed form. Some caution needs to be exercised when the derivatives of the arguments of the Airy functions with respect to R are found. As an example,

$$\frac{\partial a}{\partial R} = -\left(\frac{k_0}{A}\right)^{2/3}\left(A\left(\frac{z - z_s}{R}\right) - |A|\right)\Big/ 2 \tag{A9}$$

which still has the same form as $\partial a^i/\partial R$ when evaluated at the horizontal surface. Therefore, the entire expression inside the curly bracketts in Eq. (A8) can be labelled as $h(R, a(A), b(A))$ for convenience. Superposition for the new image source at $\boldsymbol{r}_s^i$, as previously discussed, with the original source results in

$$\frac{\partial G^*}{\partial n} = \frac{\exp(i\pi/6)}{2}\left\{\frac{\partial R}{\partial n}h(R, a(A), b(A)) + \frac{\partial R^i}{\partial n}h(R^i, a^i(-A), b^i(-A))\right\} \tag{A10}$$

which goes to zero at the horizontal surface in view of Eq. (A5) and of the fact that

$$h(R, a(A), b(A)) = h(R^i, a^i(-A), b^i(-A)) \quad \text{at} \quad z = 0. \tag{A11}$$

References

Adomian, G. (1983): Stochastic systems. New York: Academic Press
Askar, A.; Cakmak, A. S. (1988): Seismic waves in random media. Prob. Eng. Mech. 3, 124–129

Barucha-Reid, A. T. (1972): Random integral equations. New York: Academic Press
Bagtzoglou, A. C. (1990): Particle-grid methods with application to reacting flows and reliable solute source identification. Ph.D. dissertation, University of California, Irvine, California
Benaroya, H.; Rehak, M. (1987): The Neuman series/Born approximation applied to parametrically excited stochastic systems. Prob. Eng. Mech. 2, 74–81
Burczynski, T. (1985): The boundary element method for stochastic potential problems. Appl. Math. Mod. 9, 189–194
Chernov, L. A. (1962): Wave propagation in a random medium. New York: Dover
Chu, L.; Askar, A.; Cakmak, A. S. (1981): Earthquake waves in a random medium. Int. J. Num. Anal. Meth. Geomech. 5, 79–96
Cruse, T. A.; Burnside, O. H.; Wu, Y. T.; Polch, E. Z.; Dias, I. B. (1988): Probabilistic structural analysis methods for select space propulsion system structural components (PSAM). Comput. Struct. 29, 891–901
Dagan, G. (1989): Flow and transport in porous formations. Berlin, Heidelberg, New York: Springer
Dias, J. B.; Nagtegaal, J. C. (1986): Efficient algorithms for use in probabilistic finite element analysis. In Burnside, O. H.; Parr, C. H. (eds), Advances in Aerospace Structural Analysis, Vol. AD-09, pp. 37–49, New York: ASME Publication
Drewniak, J. (1985): Research communication: boundary elements for random heat conduction problems. Eng. Anal. 2, 168–169
Holford, R. L. (1981): Elementary source-type solutions of the reduced wave equation. J. Acoust. Soc. Am. 70, 1427–1436
Hryniewicz, Z. (1991): Mean response to distributed dynamic loads across the random layer for anti-plane shear motion. Acta Mech. 90, 81–89
Ishimaru, A. (1978): Wave propagation and scattering in random media, Vols. 1 and 2. New York: Academic Press
Karal, F. C.; Keller, J. B. (1964): Elastic, electromagnetic and other waves in a random medium. J. Math. Phys. 5, 537–549
Kohler, W.; Papanikolaou, G.; White, B. (1991): Reflection of waves generated by a point source over a randomly layered medium. Wave Motion 13, 53–87
Kotulski, Z. (1990): Elastic waves in randomly stratified medium. Analytical results. Acta Mech. 83, 61–75
Lafe, O. E.; Cheng, A. H. D. (1987): A perturbation boundary element code for steady-state groundwater flow in heterogeneous aquifers. Water Resour. Res. 23, 1079–1084
Li, Y. L.; Liu, C. H.; Franke, S. J. (1990): Three-dimensional Green's function for wave propagation in a linearly inhomogeneous medium – the exact analytic solution. J. Acoust. Soc. Am. 87, 2285–2291
Liu, K. C. (1991): Wave scattering in discrete random media by the discontinuous stochastic field method, I: Basic method and general theory. J. Sound Vibr. 147, 301–311
Liu, W. K.; Belytschko, T.; Mani, A. (1986): Random field finite elements. Int. J. Num. Meth. Eng. 23, 1831–1845
Luco, J. E.; Wong, H. L. (1986): Response of a rigid foundation to a spatially random ground motion. Earthquake Eng. Struct. Dyn. 14, 891–908
Manolis, G. D.; Beskos, D. E. (1988): Boundary element methods in elastodynamics. London: Chapman and Hall
Manolis, G. D.; Shaw, R. P. (1990): Random wave propagation using boundary elements. In: Tanaka, M.; Brebbia, C. A.; Shaw, R. P. (eds): Advances in boundary element methods in Japan and USA, Topics in Engineering, Vol. 7. Southampton: Computational Mechanics Publications
Manolis, G. D.; Shaw, R. P. (1992): Wave motion in a random hydroacoustic medium using boundary integral/element methods. Eng. Anal. Bound. Elem. 9, 61–70
McLachlan, N. W. (1954): Bessel functions for engineers. Oxford: Clarendon Press
Mindlin, R. D. (1936): Force at a point in the interior of a semi-infinite solid. J. Phys. 7, 195–202
Pai, D. M. (1991): Wave propagation in inhomogeneous media: a planewave layer interaction method. Wave Motion 13, 205–209
Pais, A. L.; Kausel, E. (1990): Stochastic response of rigid foundations. Earthquake Eng. Struct. Dyn. 19, 611–622
Pekeris, C. L. (1946): Theory of propagation of sound in a half-space of variable sound velocity under conditions of formation of a sound zone. J. Acoust. Soc. Am. 18, 295–315
Shaw, R. P. (1991): Boundary integral equations for nonlinear problems by the Kirchhoff transformation. In: Brebbia, C. A.; Gipson, G. S. (eds): Boundary Elements XIII, pp. 43–57. London: Elsevier
Shaw, R. P.; Makris, N. (1991): Green's functions for Helmholtz and Laplace equations in heterogeneous media. In: Brebbia, C. A.; Gipson, G. S. (eds): Boundary Elements XIII, pp. 59–69. London: Elsevier
Shinozuka, M. (1972): Digital simulation of random processes and its applications. J. Sound Vibr. 25, 111–128
Spanos, P. D.; Ghanem, R. (1991): Boundary element formulation for random vibration problems. J. Eng. Mech. ASCE 117, 409–423
Sobczyk, K. (1976): Elastic wave propagation in a discrete random medium. Acta Mech. 25, 13–28
Varadan, V. K.; Ma, Y.; Varadan, V. V. 1985): Multiple scattering theory for elastic wave propagation in discrete random media. J. Acous. Soc. Am. 77, 375–389
Vanmarke, E.; Shinozuka, M.; Nakagiri, S.; Schueller, G. I.; Grigoriu, M. (1986): Random fields and stochastic finite elements. Struct. Safety 3, 143–166
Vrettos, C. (1990a): Dispersive SH-surface waves in soil deposits of variable shear modulus. Soil Dyn. Earthquake Eng. 9, 255–264
Vrettos, C. (1990b): In-plane vibrations of soil deposits with variable shear modulus: I. Surface waves, and II. Line load. Int. J. Num. Anal. Meth. Geomech. 14, 209–222 and 649–662
Vrettos, C. (1991a): Forced anti-plane vibrations at the surface of an inhomogeneous half-space. Soil Dyn. Earthquake Eng. 10, 230–235
Vrettos, C. (1991b): Time-harmonic Boussinesq problem for a continuously non-homogeneous soil. Earthquake Eng. Struct. Dyn. 20, 961–977

Communicated by D. Beskos, May 10, 1992